Prof Suomi

PRELIMINARY

Preliminary Report on a

Cloud Statistics Study

by

Alfred Stamm

Space Science and Engineering Center
The University of Wisconsin
1225 West Dayton Street
Madison, Wisconsin 53706

June 18, 1969

Prepared Under NASA Contract NAS5-11542

Introduction

There is increasing interest today in detecting, from satellites, radiation that is reflected or emitted from the earth. In order to see the earth, a satellite must look between the clouds, but there is very little information as to how big or how frequent the cloudless areas are.

One important example of needed information on this subject is the proposed geosynchronous meteorological satellite (SMS). In addition to observing cloud patterns and motions, meteorologists are interested in sounding the atmosphere to determine a vertical temperature profile. In order to determine this profile down to the ground, they must look in cloudless areas, but the most interesting weather occurs where there are clouds. Since a number of readings are needed for "good statistics", they need to know what percentage of the area near various cloud patterns is cloudless. Also needed is information on the size of the cloudless areas or rather what instrument spatial resolution is needed to see between the clouds. This is because a tradeoff must be made between the spatial resolution and the sensitivity of the instrument.

Scientists in the Earth Resources Technology Satellite (ERTS) program are interested in looking at certain areas of the earth with various sun angles and at various times of the year. Before a program can be set up, information will be needed on the clouds covering these areas at the times of interest, especially areas that are cloudy most of the time. Such questions as: "can the information be obtained by looking between the clouds, or are cloudless days needed," and "what is the likelihood of a cloud cover at various times of the day and year," will need to be answered.

A third possible need for cloud statistics data could be in determining the types of clouds by correlating the cloud brightness and variance in brightness with cloudless area.

One of the best data sources for cloud information today is Applications Technology Satellites. An ATS-III picture is made up of 2400 lines (ATS-I has 2000 lines because the earth's poles are not included) with 8000 elements per line. Each element is assigned one of 256 brightness levels, giving a wide dyanmic range. This information has been used in various ways (as described in the following sections) to investigate the previously mentioned problems. So far, this author's research has been aimed at the SMS problems, but all of the above problems are related and should be considered together.

DEFINITIONS

Before the various methods of attacking these problems are described, a few terms should be defined as they are used in this paper. A data unit is the area which corresponds to the spatial resolution or instantaneous field of view (IFOV) of the future instrument. A basic unit is the smallest almost square area obtainable from ATS data, that is, one line by three elements or roughly 4.6 km north to south at nadir and slightly less east to west. These basic units can then be combined so that the units are made up of 1, 4, 9, 16, 25, or 36 basic units. (The linear dimension is multiplied by 1, 2, 3, 4, 5, or 6). The respective unit areas at nadir are then 21.2, 84.6, 190.6, 338.4, 529 and 1298 km^2. A grid or field is the area over which the statistics is done and is either 60 or 100 basic units on a side corresponding to 276 km and 460 km at nadir respectively. The former size was chosen because it is divisible by 1, 2, 3, 4, 5, and 6 and the latter because parallel work had

been done on the picture of interest using this size grid. Finally, a matrix is that combination of grids covering the particular cloud pattern of interest.

THRESHOLDS

As mentioned before, each element has 256 possible brightness values. Clouds are almost always brighter than either land or water but the question is: "How much brighter?" Cirrus and other type clouds may be quite dark so that determining the cloud-no cloud threshold is difficult.

A combination of two methods has been used so far in this research. First a plot of brightness versus element number is made for a given line. By locating this line on the corresponding picture, the elements which represent cloudless land and ocean values are then determined. The upper values of clear land and ocean are then read off the line plot. Figure 1 shows a typical line plot giving values for both the green and blue channels of ATS-III. So far cloud statistics studies have been made only with data from the green channel; however, anticipating that the blue channel data may be useful, thresholds have been studied in both channels. A preliminary comparison is as follows:

1. Land and ocean brightness are about the same in the blue channel.
2. Ocean is darker than land in the green channel.
3. Brightness spread is less over ocean than over land in both channels.
4. When gains are normalized to the clouds, dynamic range of green channel is greater than that of blue channel.

The larger dynamic range of the green channel makes it more promising for

cloud studies, but the blue channel might be investigated further, because of the greater land-ocean similarity.

The second method of determining the cloud-no cloud threshold is to plot the frequency at which a given brightness value occurs within a grid versus the brightness value. If there is a reasonable amount of clear area within the grid, a large peak of roughly gaussian shape will represent this clear area. The point at which the curve starts to rise again or a few brightness levels to the cloudy side of this clear area peak is taken as the point where cloud interference is becoming important. This point has been chosen as the threshold. (See Figure 2.)

At this time it should be mentioned that when the analog data was digitized, there were problems of bits "sticking." This data reduction problem affects all types of threshold criteria; it is discussed in Appendix A.

In summary, cloud-no cloud thresholds can be determined from several methods. Two of the most basic have been used in this work. Particularly over land areas the frequency distribution technique is difficult; thus more reliance was placed on the line plot displays in selecting a threshold over land areas. In all cases, a conservative estimate of the thresholds was attempted. (ie. when in doubt, the threshold was chosen to overestimate the cloudy regions.)

METHODS

The problem for SMS may be stated as follows: What percentage of the different size data units within a grid are cloudfree? Three methods of

attacking this problem have been used so far; in order of increasing stringency they are as follows:

1. When enough basic units within contiguous area equal to the area of a data unit are below the threshold, the unit "equivalent" area is counted.
2. When the average of all the elements within a data unit is below the threshold, the data unit is counted.
3. When every element within a data unit is below the threshold, the data unit is counted.

The first method was accomplished by adding together all of the basic units below the threshold within a given open area and then dividing by the number of basic units per data unit. In this case the "equivalent" units have the proper area but they are not rectangular and may even have holes in them. This obviously does not approximate the instantaneous field of view of an instrument so the method was abandoned in favor of the following methods.

The second method uses square data units and takes the average brightness of all of the elements within the data unit. This is exactly what an instrument does within its IFOV, but the question of whether there are any clouds within the unit is unanswered because a dark cloud may be averaged with a dark cloudless area and called cloudless.

Since the main problem is finding the clouds (contaminants) rather than approximating an instrument, a third method was tried. This involved setting every brightness value over the threshold to a fictitious value of one million and then proceeding as in method two. The problem of calling small dark clouds clear is thus

almost eliminated because the averaging is done over a much smaller area (ie. an ATS element).

In the following discussion of results, a comparison between the second and third methods gives some insight as to how an actual instrument (including of course, the ATS sensor) may erroneously flag an area as cloudfree, when clouds smaller than the IFOV are present.

RESULTS

April 23, 1968 (picture no. 171410z) and January 20, 1968 (picture no. 191131z) were chosen for this study. The grids for which the results are listed in this paper are in matrices 3 and 5 and part of matrix 1 of figure 3 and fields 37-40, 79-81, 83-85, and 87-95 of figure 4. Table 1 gives the percentage clear area for methods 2 and 3 for each of the grids mentioned above, with the method 2 percentages given in parenthesis. As might be expected, the open areas of method 3 fall off much faster with decreasing resolution than those of method 2. (See Figures 4 and 6). This is because some cloudy areas are included with the clear areas in method 2 due to the averaging problem. Figures 7 and 8 show what the clear areas look like for the case of a frontal zone (Field 92) and a high pressure cumulus and stratus zone (Field 85) using method 3. If this had been done for method 2, not all of the 9.2 km resolution cloudy area would have been within the 18.4 km resolution cloudy area and the 4.6 km resolution area within the 9.2 km resolution area. Figures 9-14 compare the various grids using the clear areas of method 3 normalized to the clear area at 4.6 km resolution for each grid. Figures 9-12 compare the grids within a matrix and figures 13 and 14 compare grids of roughly the same percent clear area. Figures 15 and 16 compare the averages of the above cases.

SUMMARY

The present study has examined the percent of cloudfree area within defined regions. Furthermore, this parameter (percent clear area) was studied in relation to a varying IFOV of a possible satellite sensor. In addition, the regions studied included various kinds of meteorological (ie. cloud) conditions.

It is difficult to generalize the results from this relatively small sample; more work of this kind is needed. However, one result seems evident; the percent clear area in a region decreases as the spatial resolution of the sensor is decreased. This result was not unexpected. In addition, the rate of decrease of the measured parameter is increased as cloud "contaminants" smaller than the IFOV of the instrument are considered.

These preliminary results, based on real-world measurements, from one of the highest resolution sensors available to date (the ATS Multicolor Spin-Scan Cloud Camera), may be interpreted and used for various applications. In the present study, meteorologically active regions have purposely been chosen as areas of interest. This choice was made since the U. W. group is interested in assessing the ability of an infrared sounder on a geosynchronous satellite to obtain vertical temperature profiles in and near these areas of prime meteorological interest. Thus, these results will be combined with other studies of instrument design and accuracy to optimize an infrared sounding system.

Of general interest is the indication that clouds smaller than the instrument IFOV are very important. In fact, even averaging over 4.6 km by 4.6 km (the basic unit size) versus 4.6 km by 1.5 km (the ATS element size)

is significant as evidenced by the difference in percentage clear area at 4.6 km resolution for the two methods on the same grid. (See Figures 5 and 6 and Table 1). This same evidence also indicates that determining a brightness level threshold in a visible channel is not sufficient by itself to determine whether small clouds are within the instrument's IFOV. For this reason it would be worthwhile to perform similar tests with near infrared and thermal infrared data to see if some combination of threshold criteria in several spectral channels can detect cloud contamination.

APPENDIX A

At least three types of bit sticking have been observed. Figure A1 shows a line plot in which there is a predominance of powers of 2 (ie. 32, 64, 128, and 256). A 64 thus might stand for anything between 32 and 64, therefore these pictures were rejected as being unsuitable. Figure A2 shows a brightness level plot in which there is a predominance of levels divisible by 4. This indicates that the two righthand bits are sticking on zero part of the time that they should be on one. This type of picture can be used only when every four brightness levels averaged. (ie. when a dynamic range of 256/4 = 64 is adequate).

The third type of bit sticking is more subtle and occurs in most of the pictures. Certain combinations of bits number 2, 3, 4, and 5 from the right are on or off more than they should be. (In this study under a different portion of the same NASA contract the first bit was eliminated from this analysis because it was too unreliable.) For example, 0011 and 0111 occur too often and 0010 and 0101 occur too seldom. As a future refinement to the data, a correction could be made by determining how often on the average each brightness value is in error, but this would only help in determining the threshold since it would be an average correction and therefore could be used only with a large number of elements such as in the brightness level plot of figure 2. Whether or not an individual element is in error would not be known. The only realy solution to the bit sticking problem is to eliminate it at the source, (which has not been isolated yet) but for this preliminary study, the available data should be adequate.

Table 1

Percentage Clear Area Obtained by Method 3 (Method 2 data in parenthesis)

April 23, 1968 (171410Z) Matrix 1
Extratropical Front over Midwestern U.S.

Resolution at Nadir (km)	4.6	4.6	9.2	13.8	18.4	23.0	27.6
Row 4 cl 2	11.36	(12.86)	9.00 (12.67)	7.25 (12.25)	5.78 (12.89)		4.00 (12.00)
Row 4 cl 3	16.17	(20.22)	10.00 (19.00)	5.50 (18.75)	4.00 (18.67)		0 (18.00)
Row 4 cl 4	0	(0)	0 (0)	0 (0)	0 (0)		0 (0)
Row 4 cl 5	8.00	(11.22)	4.22 (10.22)	1.75 (9.75)	1.33 (8.44)		0 (8.00)
Row 5 cl 2	24.00	(26.50)	19.33 (25.67)	15.25 (25.75)	13.78 (25.33)		9.00 (24.00)
Row 5 cl 3	0.53	(0.86)	0.22 (0.67)	0 (0.50)	0 (0.44)		0 (0)
Row 5 cl 4	1.14	(2.22)	0.11 (1.33)	0 (1.50)	0 (0.89)		0 (0)
Row 5 cl 5	0	(0)	0 (0)	0 (0)	0 (0)		0 (0)

April 23, 1968 (171410Z) Matrix 3
Extratropical Front over Northwestern U.S. and Ocean

Resolution at Nadir (km)	4.6	9.2	13.8	18.4	23.0	27.6
Row 1 cl 1	80.33 (82.39)	74.22 (82.67)	67.75 (83.25)	60.89 (83.56)	56.94 (84.72)	53.00 (84.00)
Row 1 cl 2	8.92 (10.14)	6.33 (9.67)	4.75 (10.50)	3.11 (9.78)	2.08 (9.72)	1.00 (9.00)
Row 2 cl 1	18.89 (22.81)	12.67 (21.67)	9.50 (21.75)	6.67 (23.11)	5.56 (22.22)	3.00 (22.00)
Row 2 cl 2	40.53 (50.33)	23.11 (47.54)	10.25 (50.25)	4.89 (50.67)	1.39 (52.08)	0 (51.00)

April 23, 1968 (171410Z) Matrix 5
Cumulus and Cumulonimbus over Amazon

Resolution at Nadir (km)	4.6	9.2	13.8	18.4	23.0	27.6
Row 1 cl 1	9.81 (13.17)	2.44 (9.56)	0.75 (7.25)	0 (6.67)	0 (4.86)	0 (5.00)
Row 1 cl 2	9.58 (13.00)	2.89 (10.00)	0.50 (7.75)	0 (5.33)	0 (4.17)	0 (5.00)
Row 1 cl 3	12.97 (17.50)	3.11 (13.33)	0.75 (10.50)	0 (5.78)	0 (5.56)	0 (3.00)
Row 2 cl 1	41.14 (53.61)	15.44 (50.78)	6.75 (50.00)	2.22 (49.78)	1.39 (48.61)	1.00 (43.00)
Row 2 cl 2	20.11 (24.22)	10.89 (21.56)	5.75 (18.75)	4.44 (19.11)	3.47 (15.97)	1.00 (17.00)
Row 3 cl 3	12.75 (17.47)	3.89 (15.00)	0.75 (11.50)	0.44 (8.89)	0 (7.64)	0 (7.00)

Table I (con't.)

Jan. 20, 1968 (191131Z) Matrix 1
Inner Tropical Convergence Zone

Resolution at Nadir (km)	4.6	9.2	18.4
Field 37	7.85 (9.25)	5.44 (8.32)	3.04 (7.68)
Field 38	2.04 (3.06)	0.52 (2.40)	0 (1.76)
Field 39	4.06 (5.45)	1.40 (4.56)	0.32 (2.88)
Field 40	18.58 (20.82)	13.16 (19.88)	6.56 (17.28)

Jan. 20, 1968 (191131Z) Matrix 2
Subtropical High Pressure Cumulus and Stratus

Resolution at Nadir (km)	4.6	9.2	18.4
Field 79	9.33 (13.09)	2.96 (10.28)	0.32 (5.44)
Field 80	6.75 (7.70)	4.72 (7.40)	2.72 (6.72)
Field 81	40.36 (43.19)	34.32 (42.92)	27.36 (41.44)
Field 83	36.70 (42.06)	25.52 (40.60)	11.84 (37.28)
Field 84	70.54 (74.11)	60.64 (73.60)	44.64 (71.52)
Field 85	65.00 (68.46)	54.92 (67.52)	39.20 (66.08)

Jan. 20, 1968 (191131Z) Matrix 3
Extratropical Front over Southwest Pacific

Resolution at Nadir (km)	4.6	9.2	18.4
Field 87	61.15 (65.61)	50.64 (64.72)	38.08 (63.20)
Field 88	7.28 (9.49)	3.60 (7.88)	1.60 (5.60)
Field 89	27.47 (31.86)	18.40 (31.68)	9.76 (30.72)
Field 90	13.76 (19.72)	4.64 (16.40)	0.32 (13.76)
Field 91	24.20 (29.70)	13.80 (26.36)	6.24 (22.08)
Field 92	27.77 (31.72)	19.56 (30.84)	9.76 (29.44)
Field 93	0 (0)	0 (0)	0 (0)
Field 94	7.12 (8.36)	4.60 (8.00)	1.76 (6.88)
Field 95	14.60 (18.24)	8.72 (16.92)	3.52 (14.72)

Figure 1

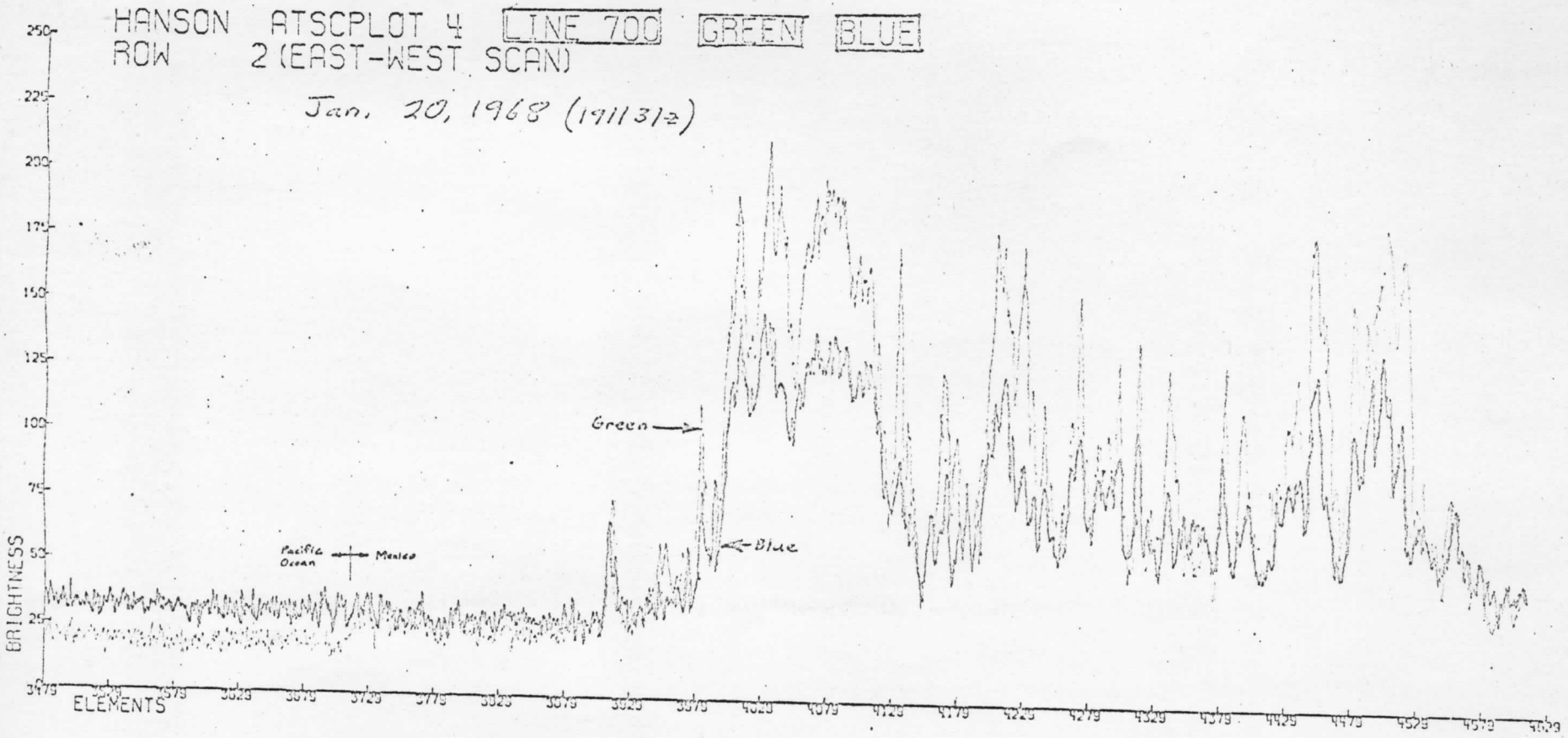
HANSON ATSCPLOT 4 LINE 700 GREEN BLUE
ROW 2 (EAST-WEST SCAN)
Jan. 20, 1968 (1911312)
BRIGHTNESS
ELEMENTS
Green
Blue
Pacific Ocean
Mexico

ATS BRIGHTNESS FREQUENCY DISTRIBUTION

Figure 2

Jan. 20, 1968 (191131Z)
Field 95

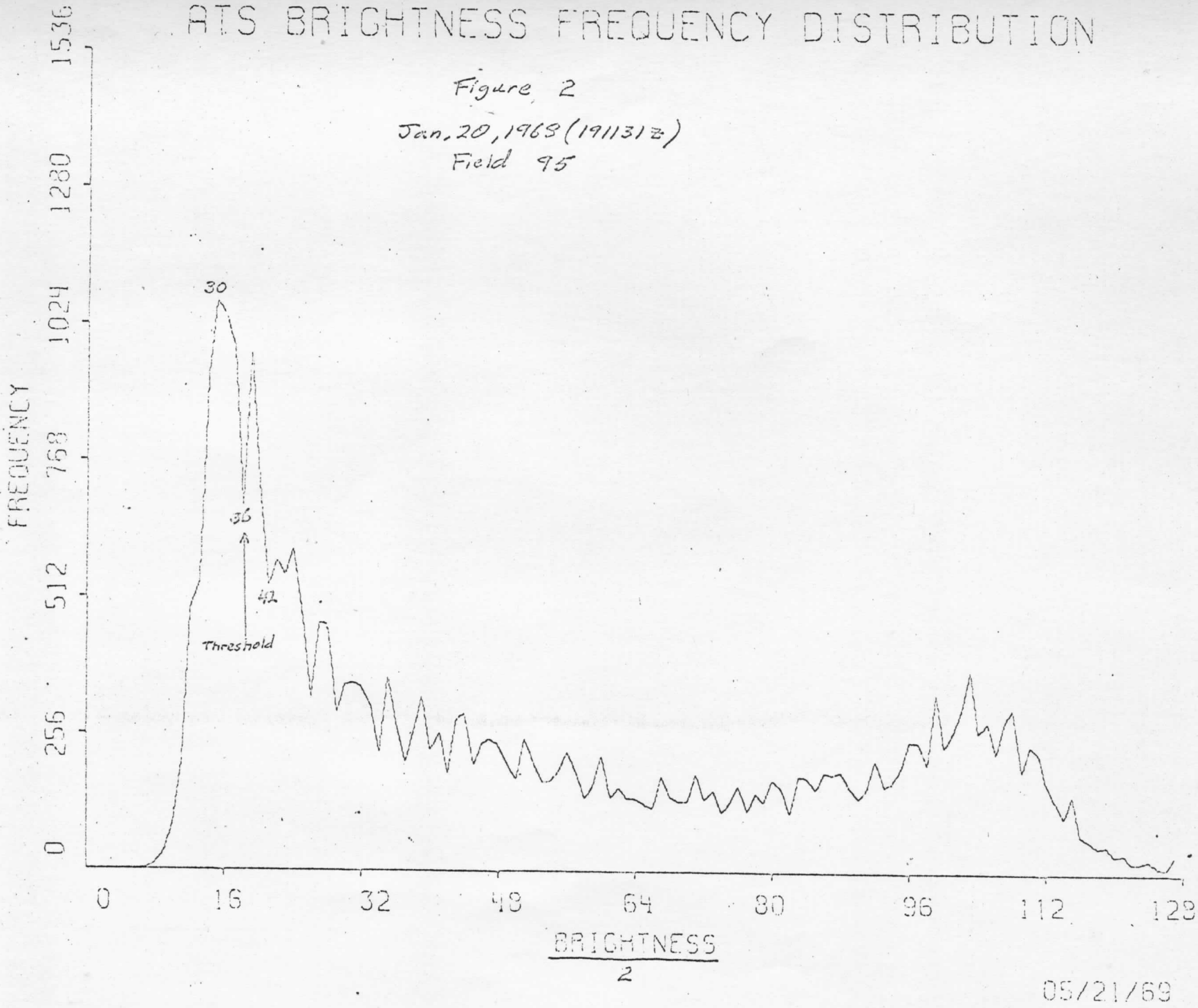

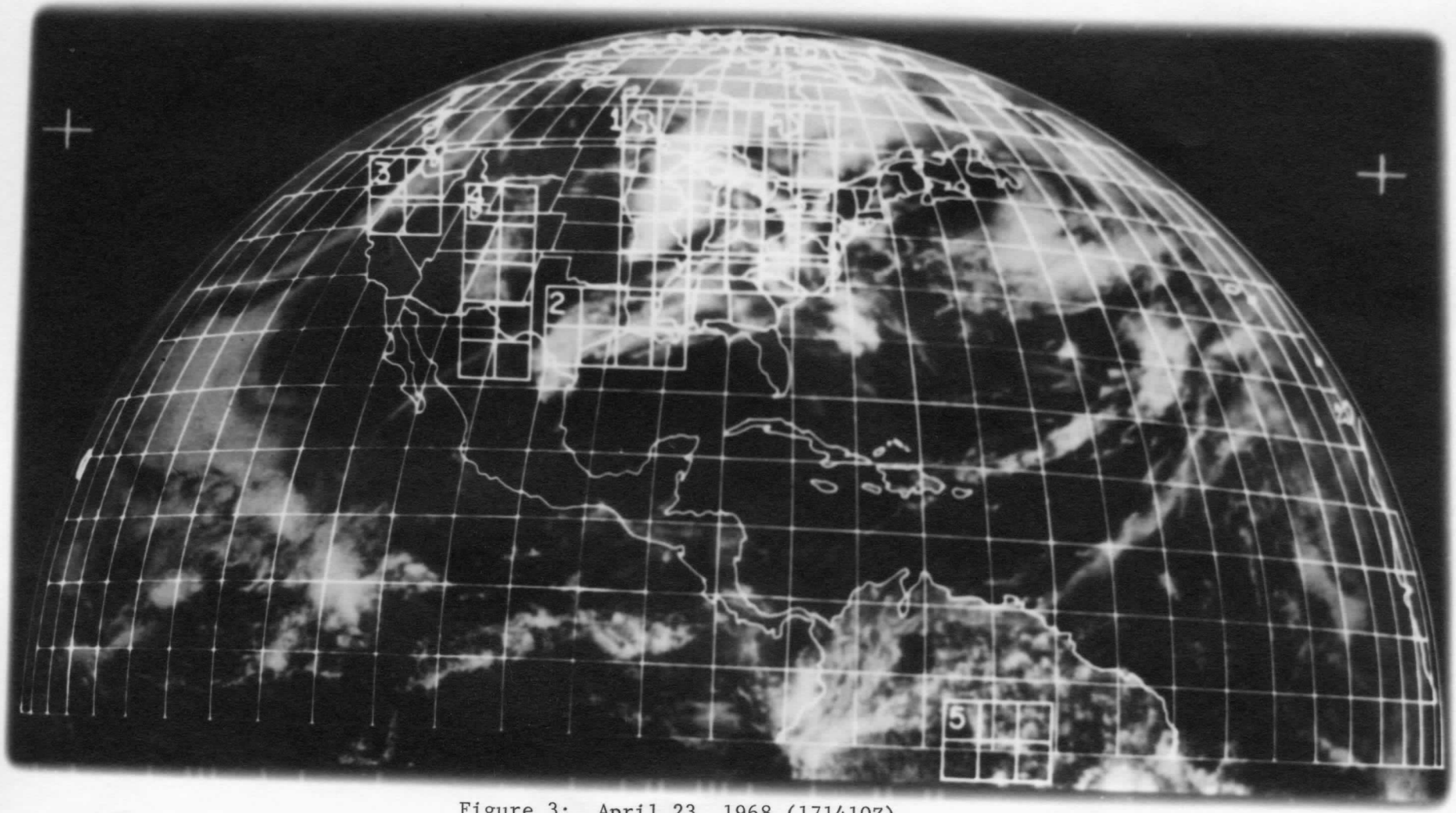

Figure 3: April 23, 1968 (171410Z)

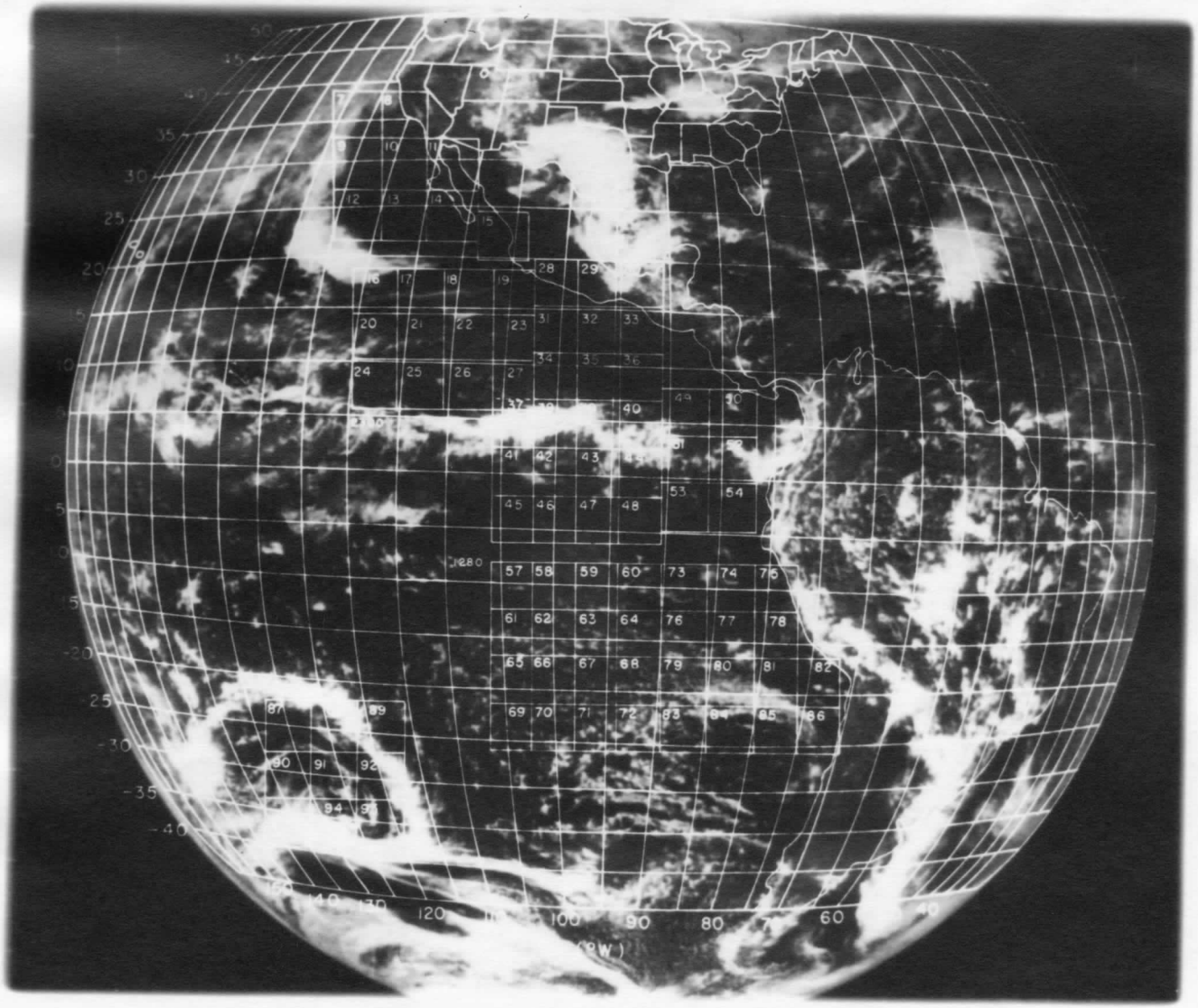

Figure 4: January 20, 1968 (191131Z)

(9)

Figure 5

Extratropical Front over Northwestern U.S.

Roman Numeral Refers to Method
Row and Column Locate Grid within Matrix

April 23, 1968 (1714102)
Matrix 1

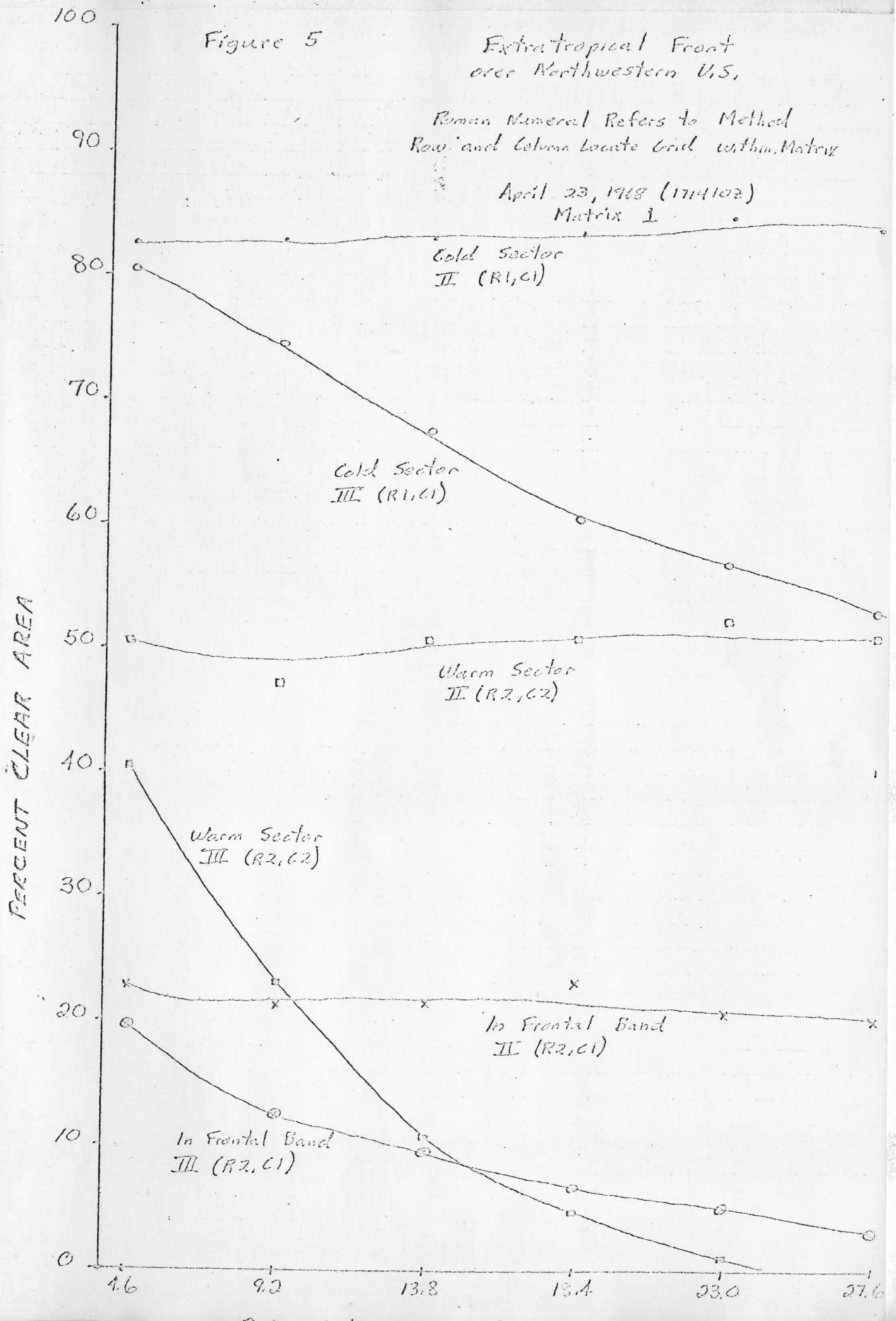

(P)

Figure 6

Cumulus and Cumulonimbus over Amazon

Roman Numeral Refers to Method
Row and Column Count Grid within Matrix

April 23, 1968 (1711-1012)
Matrix 5

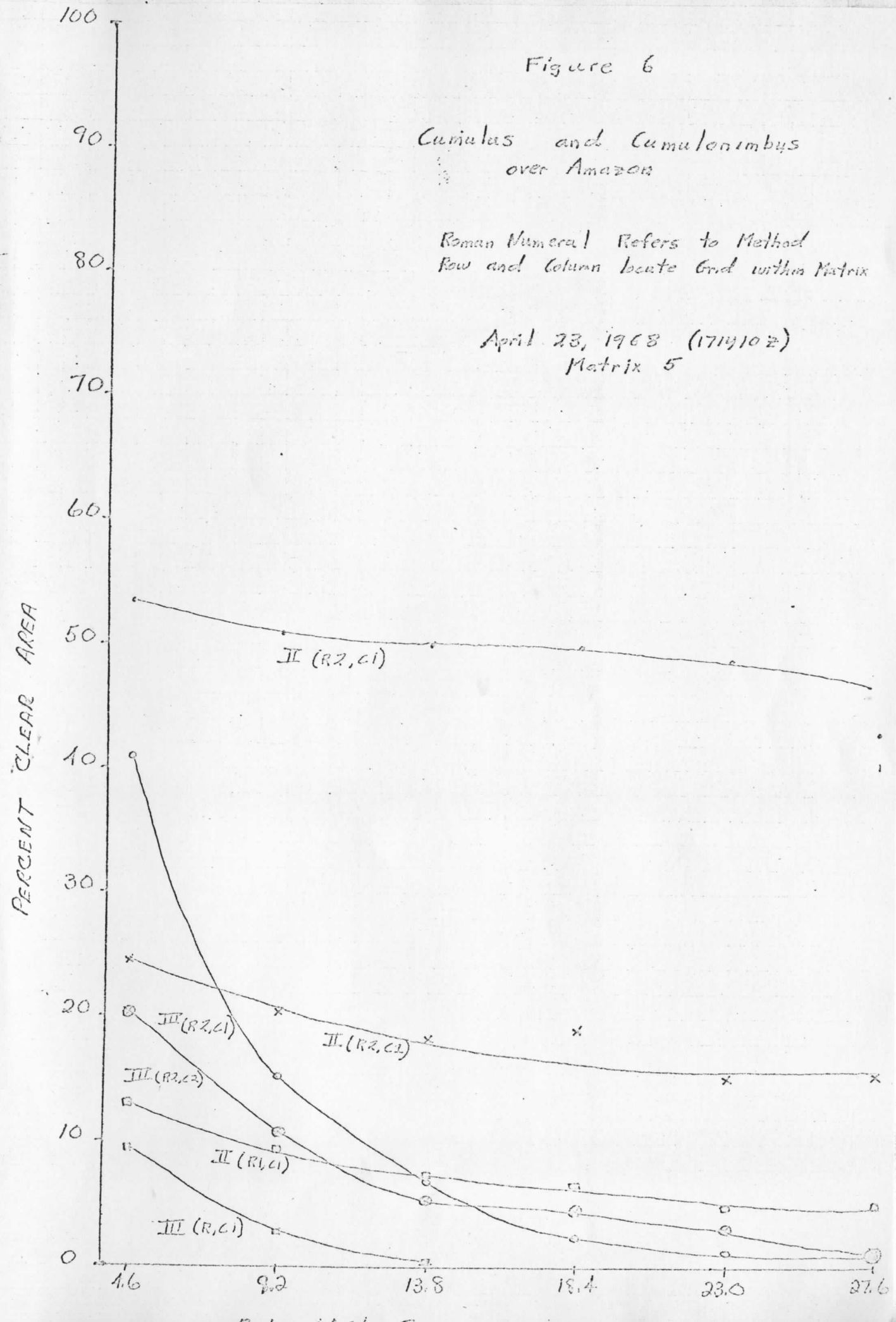

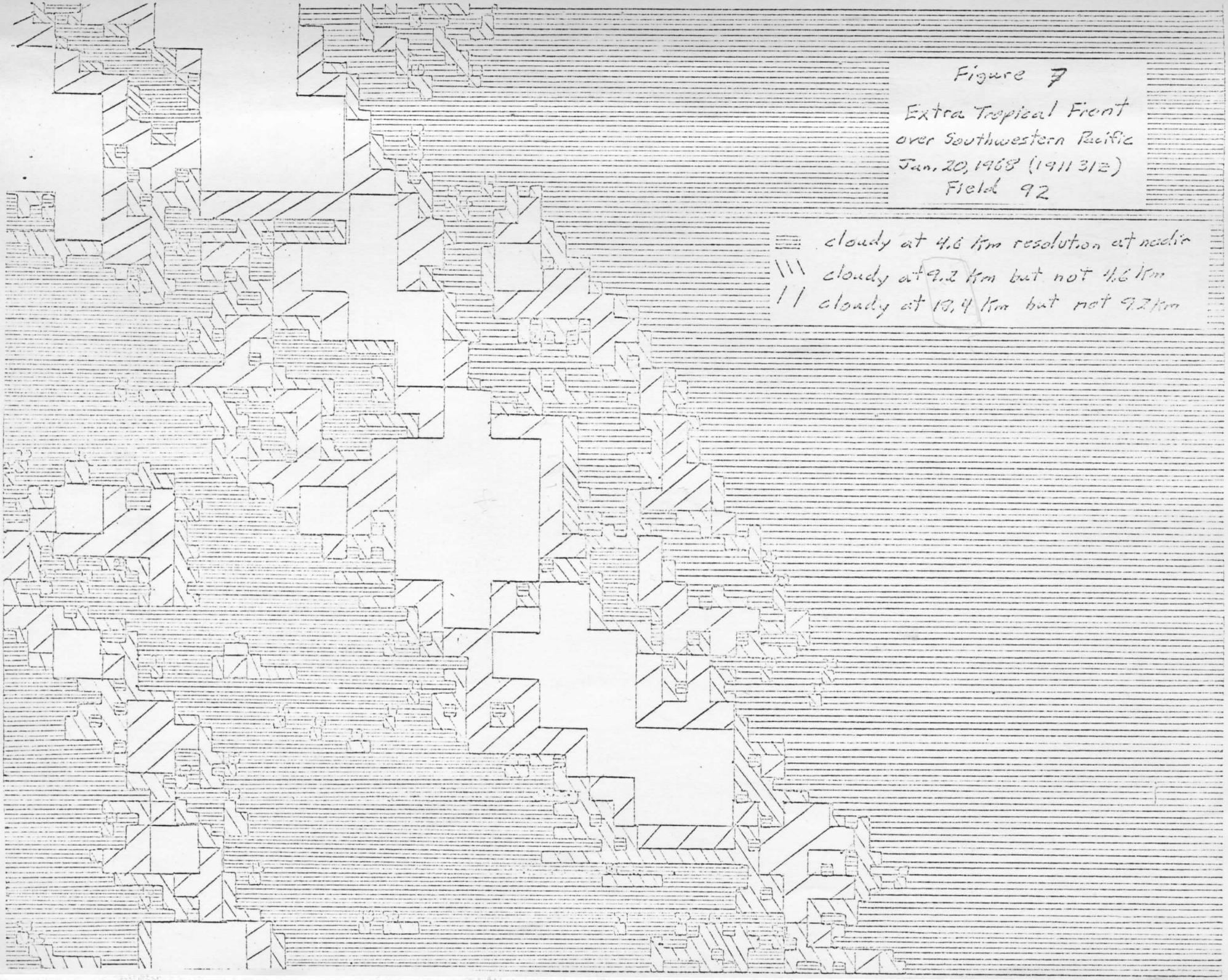

Figure 7

Extra Tropical Front over Southwestern Pacific Jan. 20, 1968 (1911312) Field 92

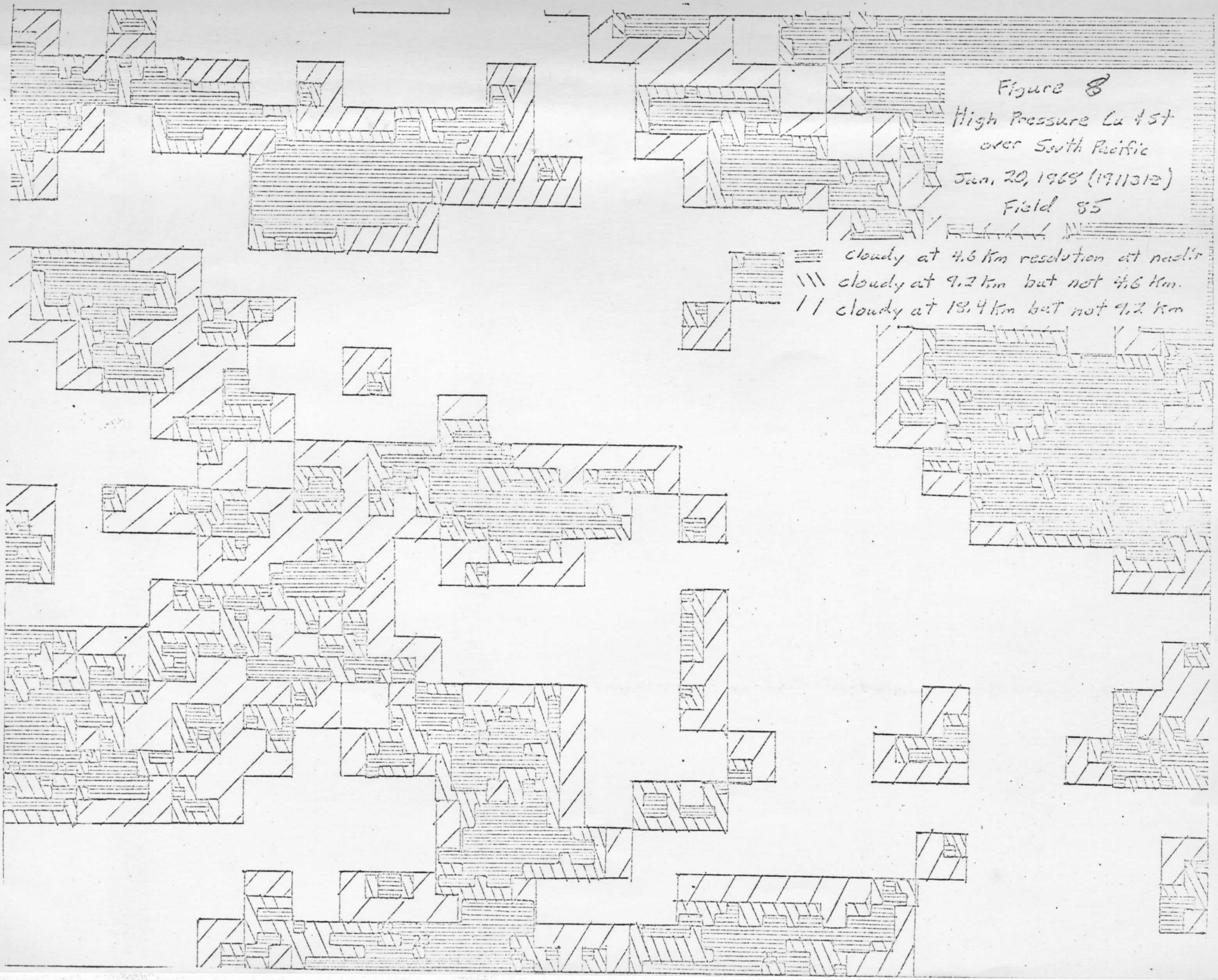
Figure 8
High Pressure Cu 45t
over South Pacific
Jan. 29, 1968 (1911312)
Field 85
cloudy at 4.6 Km resolution at nadir
cloudy at 9.2 Km but not 4.6 Km.
cloudy at 18.4 Km but not 9.2 Km

(6)

Figure 9

Extratropical Front over Northwestern U.S.

(numbers indicate percent clear area at 4.6 km. resolution at nadir)

April 23, 1968 (1714102)
Matrix 3

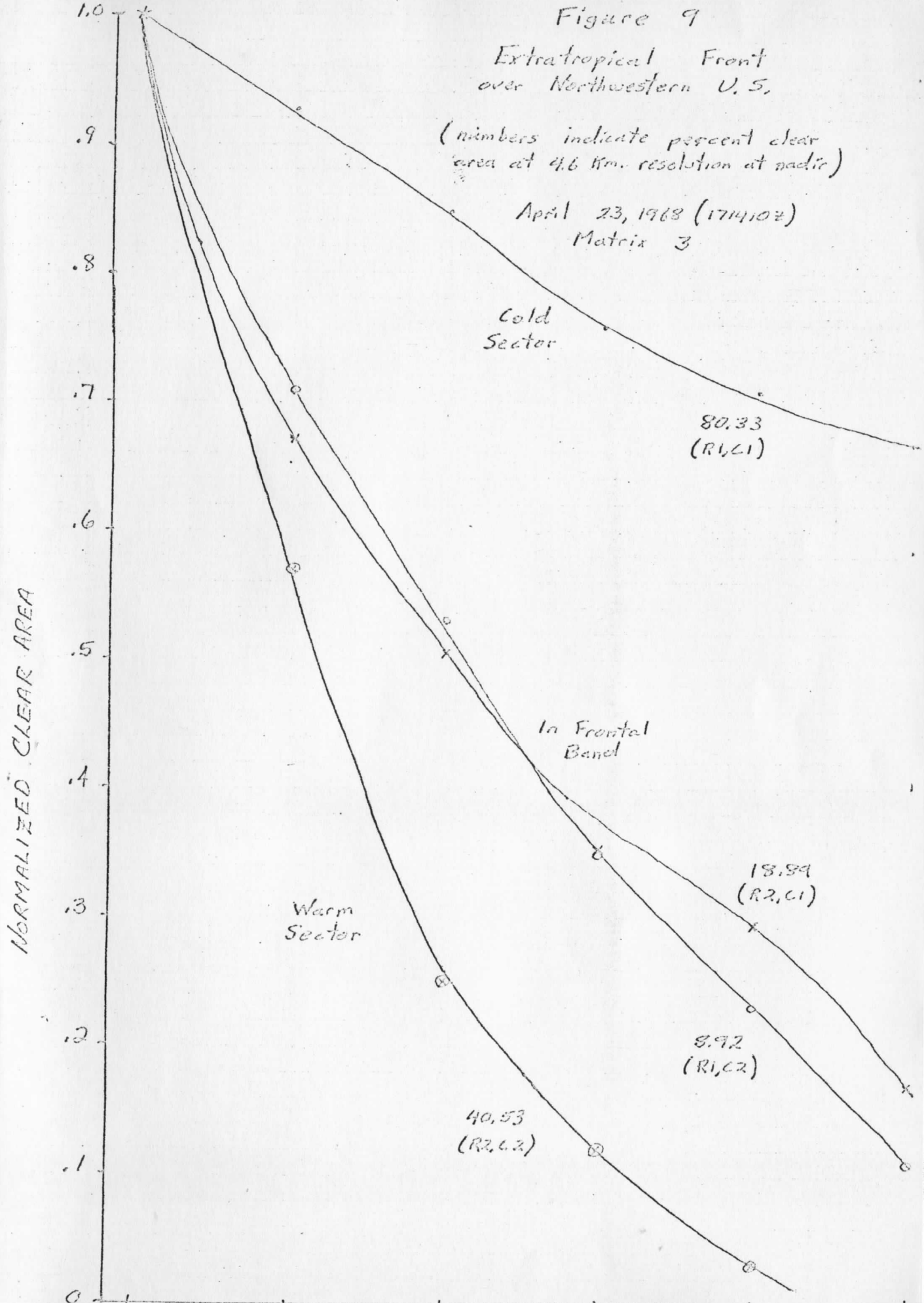

(1)

Figure 10

Inner Tropical Convergence Zone

(numbers indicate percent clear area at 4.6 km. resolution at nadir)

Jan. 20, 1968 (1911312)

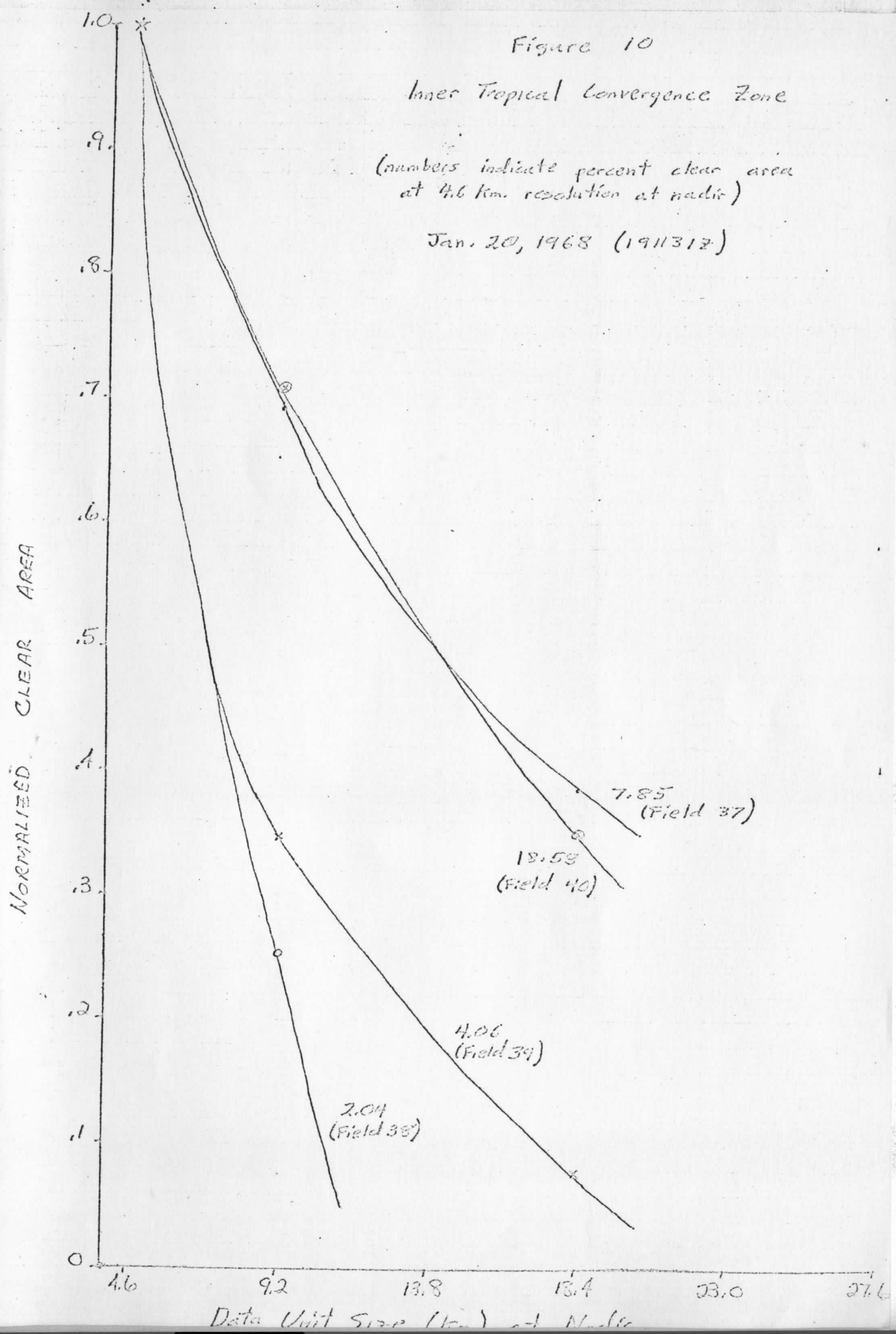

(E)

Figure 11

Subtropical High Pressure Cumulus and Stratus

(numbers indicate percent clear area at 4.6 Km. resolution at nadir)

Jan. 20, 1968 (1911312)

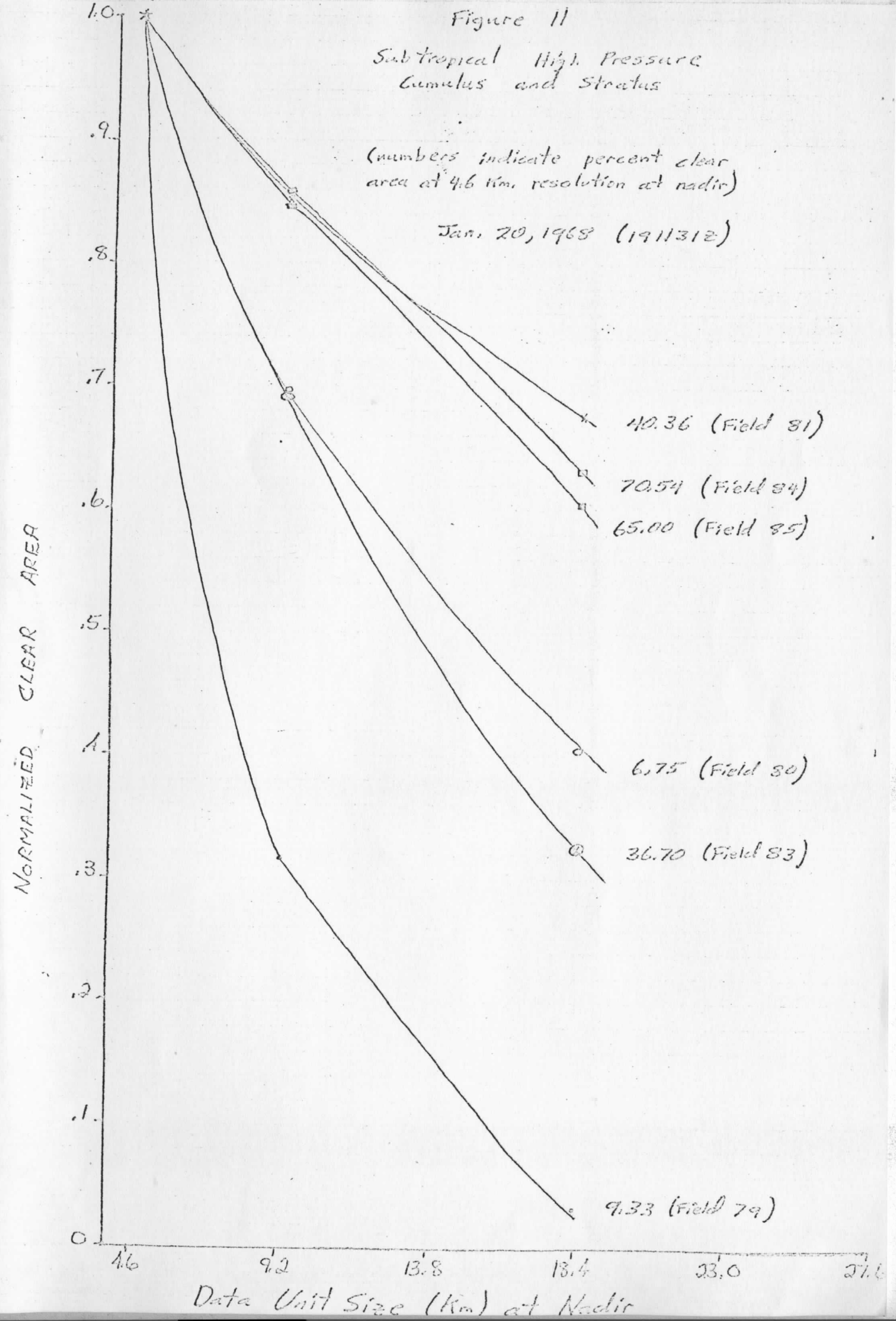

(A)

Figure 12
Extratropical Front
over Midwestern U.S.

(numbers indicate percent clear area
at 4.6 km. resolution at nadir)

April 23, 1968 (1719102)
Matrix 1

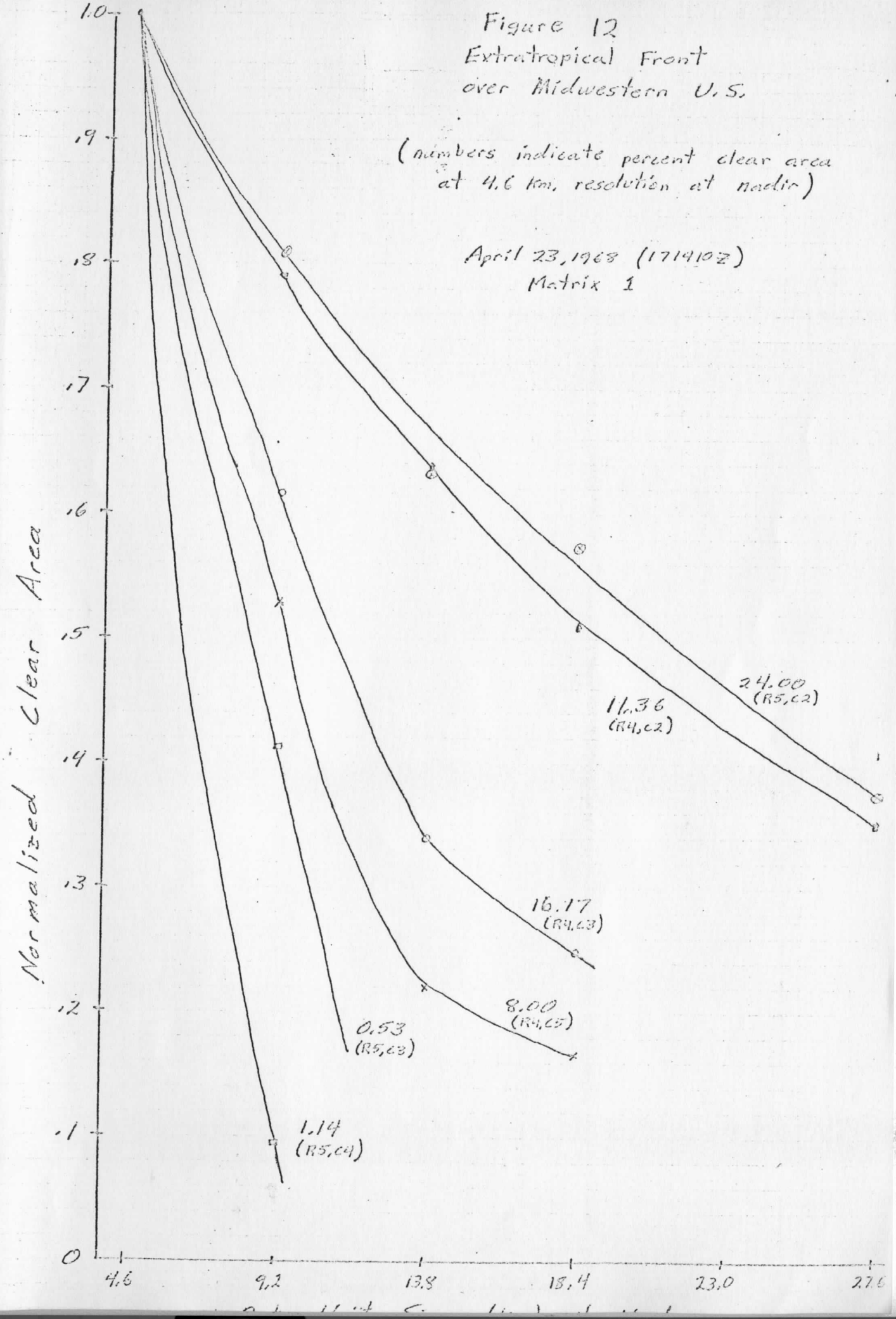

(i)

Figure 13

Percent Clear Area : 36 - 42

(numbers indicate percent clear area at 4.6 km resolution at nadir)

Jan. 20, 1968 (1911312)
April 23, 1968 (1711410)

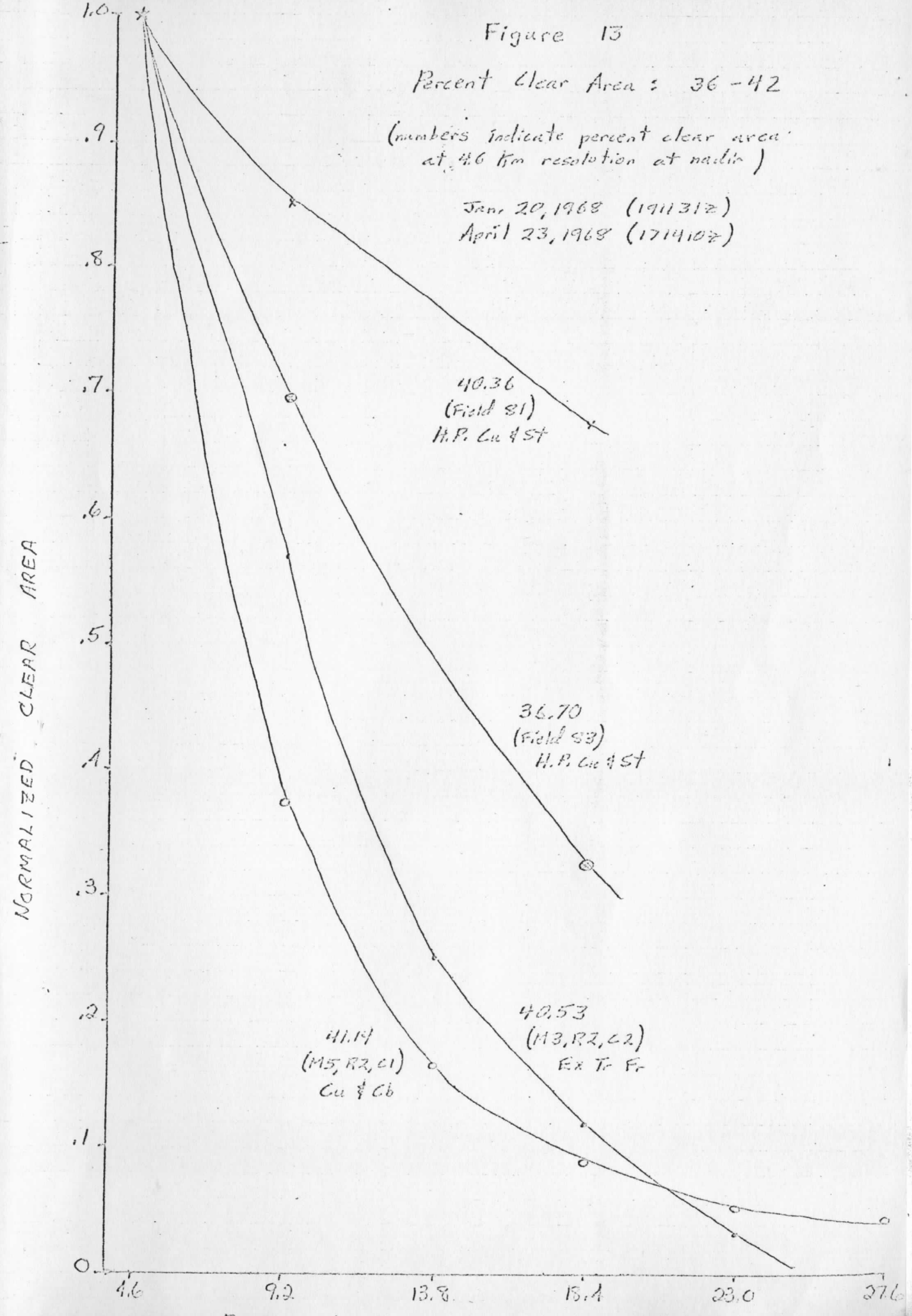

(1)

Figure 14

Percent Clear Area : 6-8

(numbers indicate percent clear area at 4.6 km resolution at nadir)

Jan. 20, 1968 (1911312)
April 23, 1968 (1714102)

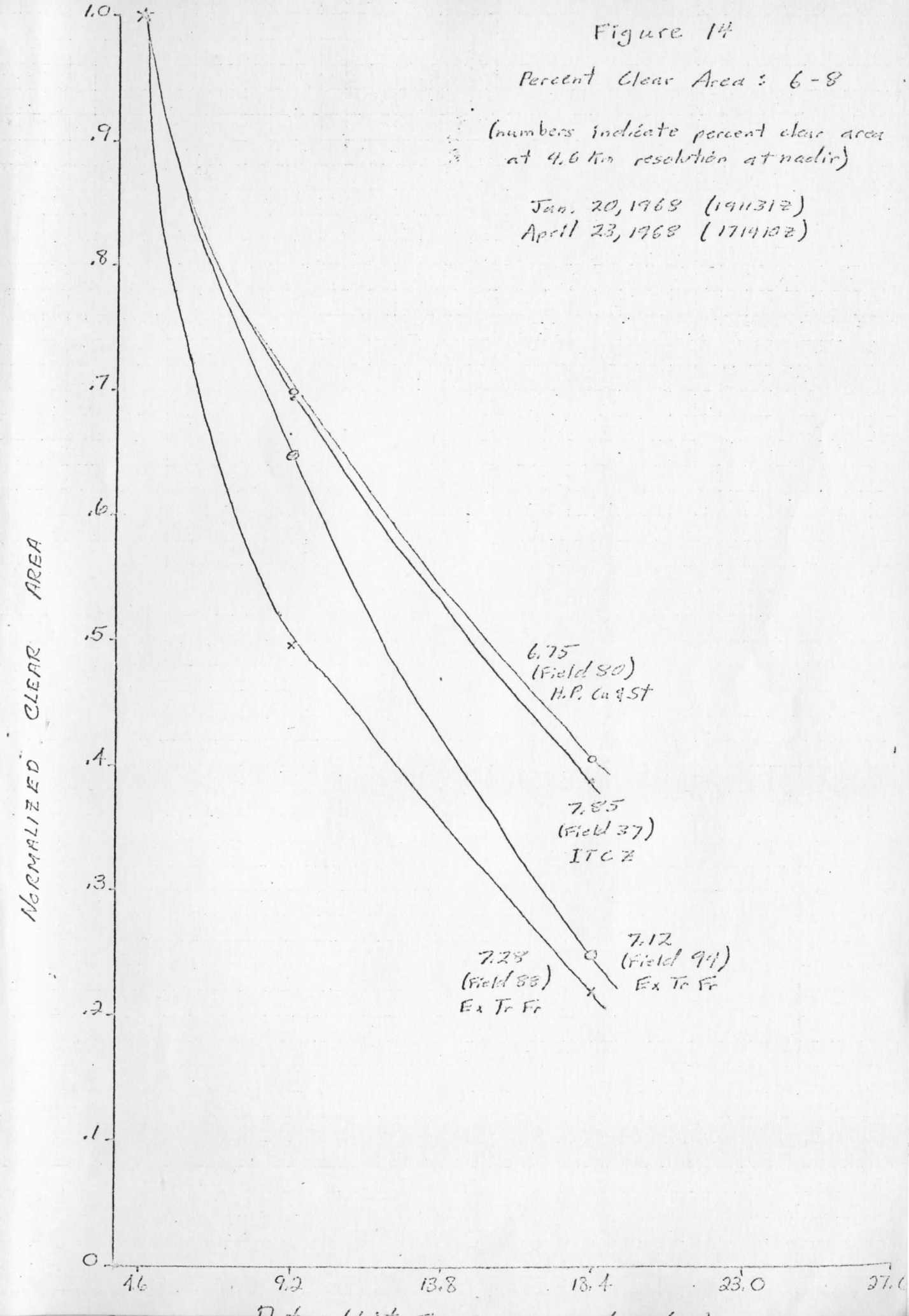

(11)

Figure 15

Average Values for each Matrix

Jan. 20, 1968 (1911312)
April 23, 1968 (1714102)

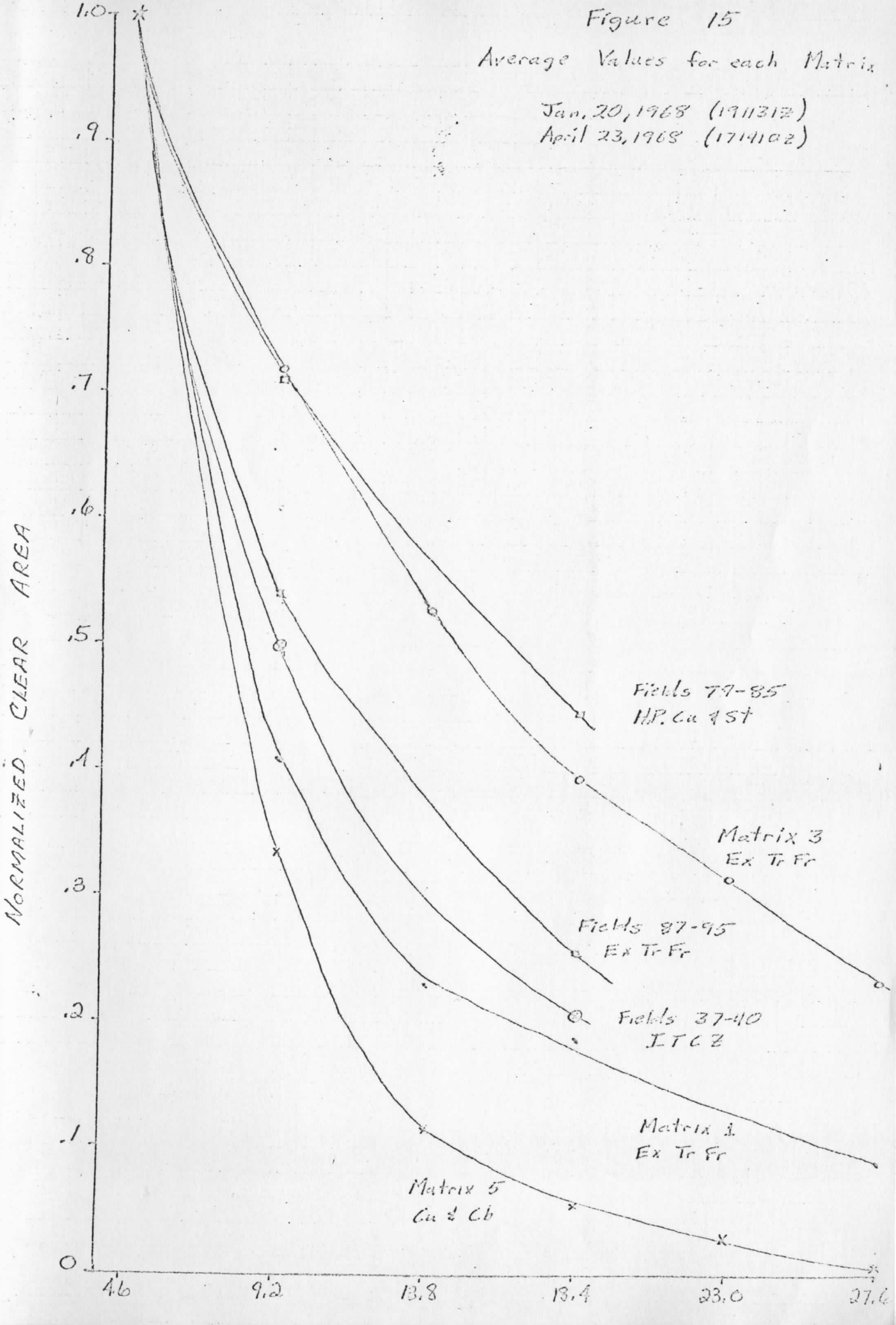

(c)

Figure 16

Average Clear Areas

(numbers indicate the range of percent clear area at 4.6 km resolution at nadir)

Jan. 20, 1968 (1911312)
April 23, 1968 (1711102)

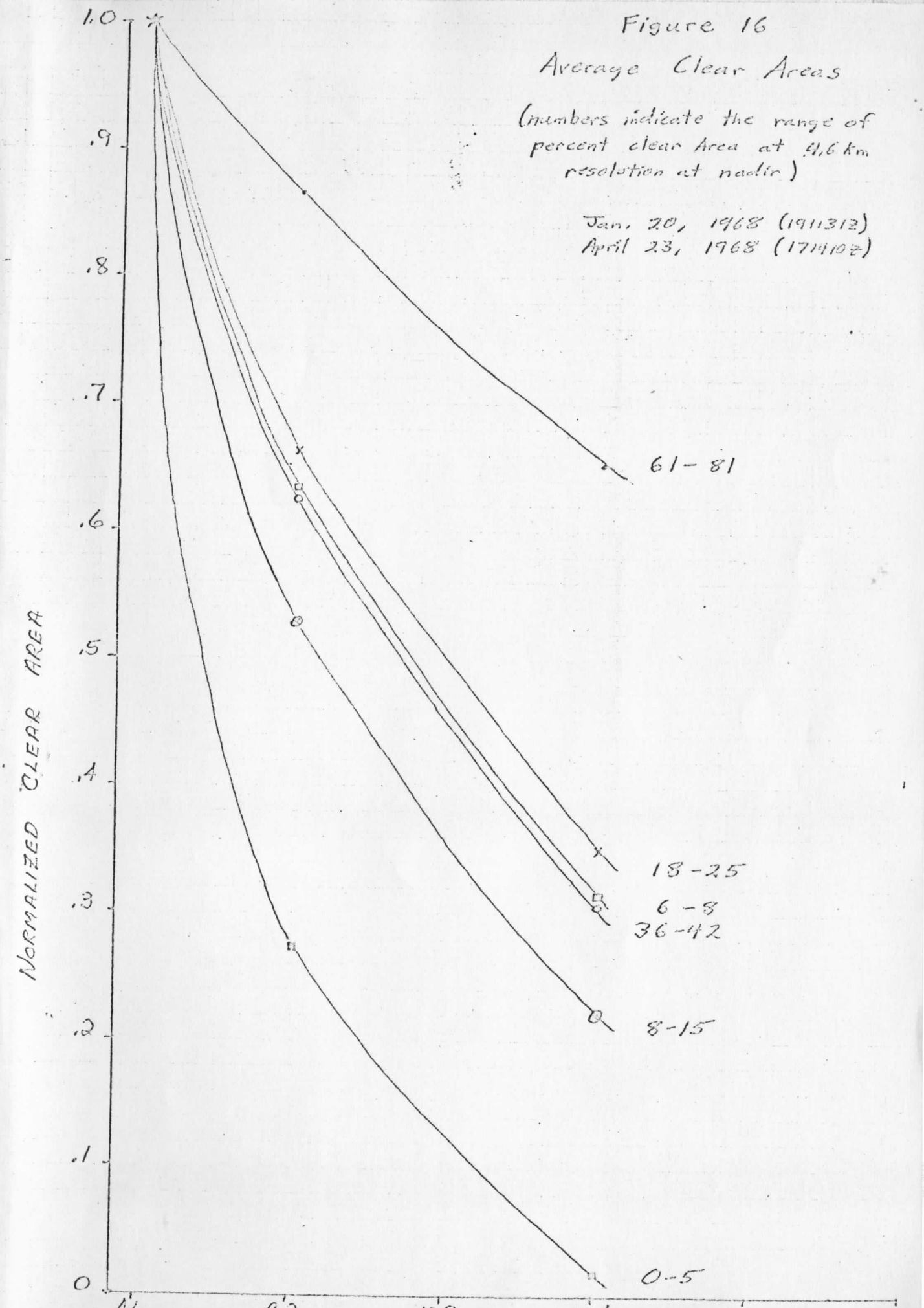

Figure A1

April 16, 1967 (106-7-201238)

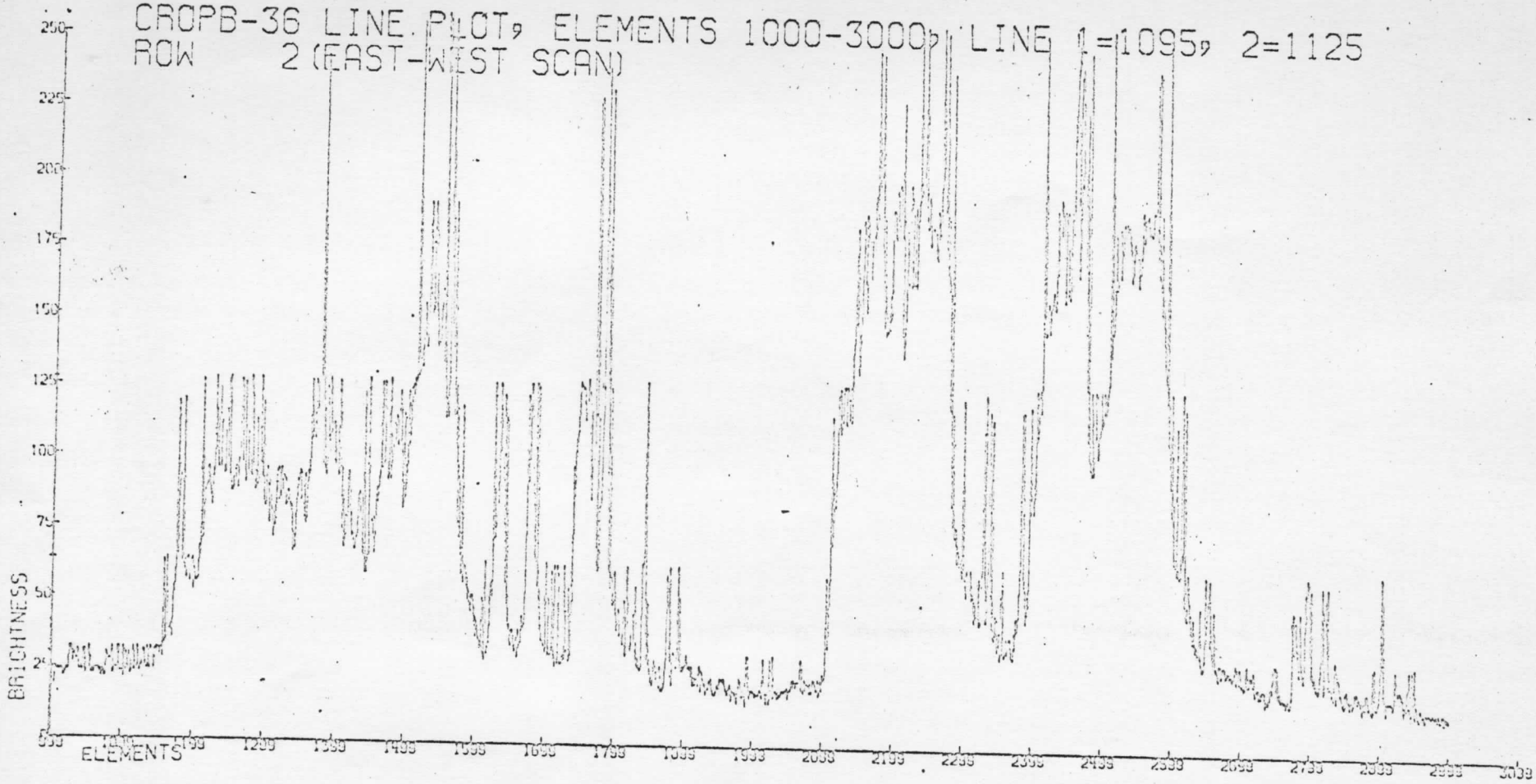

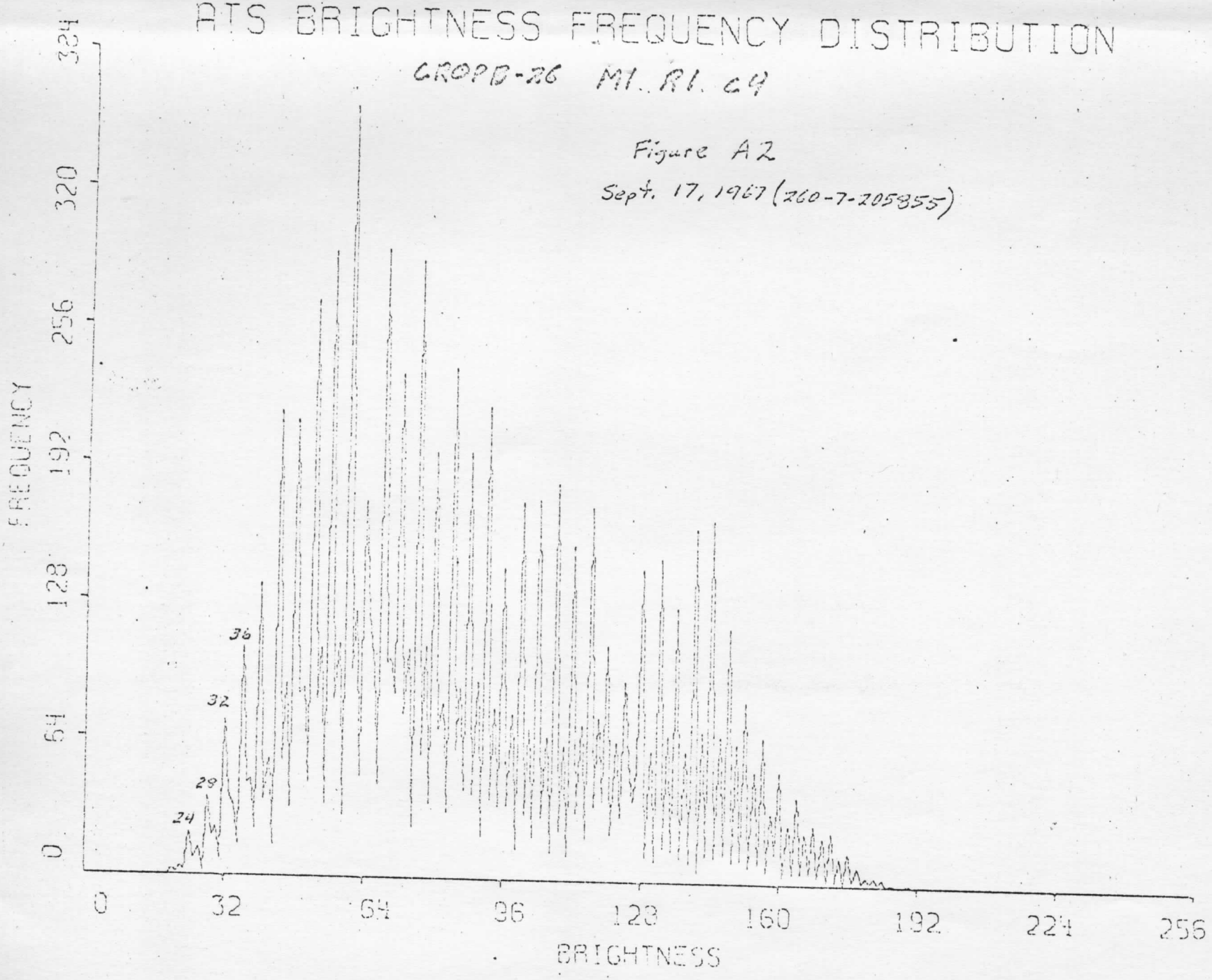

Figure A2

Sept. 17, 1967 (260-7-205855)

05/10/68